COMPARISON BETWEEN H-INFINITY CONTROL AND NONLINEAR PREDICTIVE CONTROL OF AUTOMATIC VEHICLE STEERING

Gheorghe LIVINT , Razvan C. RAFAILA
Faculty of Electrical Engineering and Applied Informatics
"Gheorghe Asachi" Technical University
Iasi, Romania
glivint@tuiasi.ro, razvan.rafaila@gmail.com

Abstract**:** *In this work a comparison between H_∞ control and Nonlinear Model Predictive Control is carried out for controlling the steering system of automated ground vehicles. A rigorous analysis between the performances of the two controllers is given, presenting advantages and drawbacks of each method, using simulation results. A detailed description of the design approaches is also given.*

Keywords: *H-infinity control; mixed sensitivity method; NMPC; autonomous vehicles; lateral control; vehicle model;*

1. Introduction

Currently, both industry and academic fields are focusing in making complete automated vehicles a reality. Both fields conduct intensive research programs, in order to find the best solutions for this challenging task. While the available computational power grows and more and more advanced control systems can be developed, the focus on passengers comfort and especially safety still remains a limiting factor in implementing automated vehicles control systems. For this reason, auto-makers try to bring the concept on the market iteratively, by adding different and increasing levels of automation of the vehicles year by year.

Research in automatic driving is ongoing for some years and functionalities of partial autonomy are already available in series production which are contributing to driver safety and comfort, and interested readers may refer to [1], [2].

Multiple control system approaches are already studied in academy and industry for the control of automatic driving vehicles, and many of them rely on advanced control techniques such as nonlinear control [3], robust control [4], [5] and model predictive control [6], [7], [8], and [9].

In this paper the mixed sensitivity design method of an H_∞ controller and a Nonlinear Model Predictive Control are proposed, for the design of automatic steering system for ground vehicles, and the obtained closed loop performances are studied in vehicle trajectory following. Comparison of the two proposed controllers is given, in controlling the vehicle lateral dynamic, considering a double lane change scenario at constant vehicle speed. The desired trajectory of the vehicle is considered already known, also it is assumed that all needed sensors for measuring the vehicle motion and actuators are available in the vehicle. Inclusion of all these aspects is subject to future contributions.

The rest of this paper is structured as follows: in Section 2. a short description of vehicle nonlinear dynamics and modelling is presented; the H_∞ control design by mixed sensitivity method is presented Section 3; the design Nonlinear Predictive Controller and the controller design for vehicle steering are given in Sections 4 and 5. Simulation results are presented in Section 6, and de conclusions are given in Section 7.

2. Vehicle Dynamics Modelling

Typically vehicle dynamics refer to vehicle motion in longitudinal and lateral directions. Longitudinal dynamics concern the vehicle behavior while accelerating, braking and traction properties of the wheels on different road surfaces under different conditions. Lateral dynamics is governed by the vehicle stability analysis, cornering and road keeping. The single-track model or bicycle model is widely used in the study of vehicle motion and control [10], [11], and is also adopted in this paper for the design and study of both control strategies. In Fig. 1, the vehicle model is represented. The dynamic model can be written using the following differential equations:

$$\begin{aligned} m\ddot{x} &= m\dot{y}\dot{\psi} + 2F_{xf} + 2F_{xr}, \\ m\ddot{y} &= -m\dot{x}\dot{\psi} + 2F_{yf} + 2F_{yr}, \\ I\ddot{\psi} &= 2aF_{yf} - 2bF_{rf}, \end{aligned} \tag{1}$$

where F_{xf} is the longitudinal force of the front wheel tire, F_{xr} is the longitudinal force of the rear wheel tire, F_{yf} is the lateral force of the front wheel tire, and F_{yr} is the lateral force of the rear wheel tire. The states of the vehicle are as follows: the longitudinal position x, the lateral position y and the yaw angle ψ. Finally m, I, a and b are the vehicle mass, vehicle inertia, distance from the front axle to the center of gravity and distance from the rear axle to the center of gravity.

It should be noted that the degrees of freedom of the nonlinear model described by (1), are considered in the vehicle coordinate system, which is centered in the vehicle's center of gravity. An inertial representation of the vehicle motion can be obtained by changing these coordinates to the inertial coordinate system.

The tire forces can be obtained by using the nonlinear Pacejka Tire Model [12], [13], using the longitudinal slip values - for calculating F_{xf}, F_{xr}, and the slip angles - for calculating F_{yf}, F_{yr}. The Pacejka Tire Model tire model also includes the influences that the normal forces acting on the front and rear axles, and describes the tire forces as:

$$\begin{aligned} F_{xf} &= f_{xf}(\alpha_f, \kappa_f, F_{zf}),\ F_{xr} = f_{xr}(\alpha_r, \kappa_r, F_{zr}), \\ F_{yf} &= f_{yf}(\alpha_f, \kappa_f, F_{zf}),\ F_{yr} = f_{yr}(\alpha_r, \kappa_r, F_{zr}), \end{aligned} \tag{2}$$

where α_f denotes the front tire slip angle, α_r is the rear tire slip angle, κ_f is the longitudinal slip of the front tire, κ_r is the longitudinal slip of the rear tire, and F_{zf}, F_{zr} are the normal forces acting on the front and rear axles. The nonlinearities that have the highest impact in the vehicle dynamics, described by equations (2), arise from the tire models, as the tire forces are highly nonlinear for high slip quantities, which can occur when the vehicle drives over slippery roads.

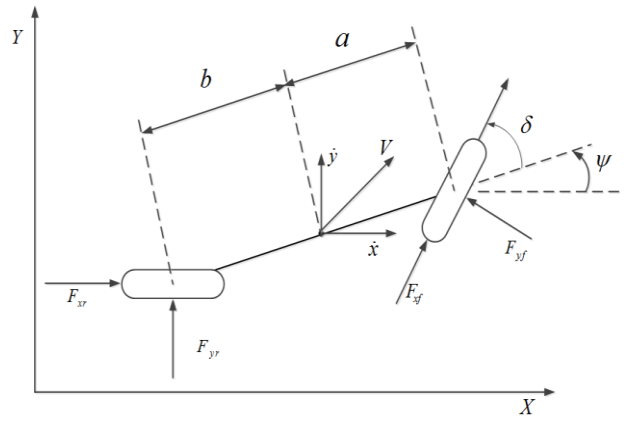

Fig. 1. Vehicle single-track model

The presented nonlinear model will be further used to validate the controller performance. For brevity, the nonlinear model will not be presented here, and interested readers may refer to [7], [8], [12] and [13] for more information regarding the vehicle nonlinear modelling.

The nonlinear vehicle model will be used for the NMPC while for the proposed H_∞ control design; a linearization of this model is done, considering constant vehicle speed. This linear model can be obtained by making linear approximations of the tire forces, of the form:

$$F_{yf} = C_{yf}\alpha_f,\ F_{yr} = C_{yr}\alpha_r, \tag{3}$$

where C_{yf} and C_{yr} represent the cornering stiffness coefficients characterizing the front and rear tires. Using small angle approximations, the tire slip angles can be calculated as:

$$\alpha_f = \delta - \frac{\dot{y} + a\dot{\psi}}{\dot{x}},\ \alpha_r = \frac{\dot{y} - b\dot{\psi}}{\dot{x}}, \tag{4}$$

where δ represents the front wheel steering angle.

Finally, considering constant vehicle speed, the nonlinear model described by (1) can be linearized to the form:

$$\begin{aligned} m\ddot{y} &= -mV_x\dot{\psi} + 2F_{yf} + 2F_{yr}, \\ I\ddot{\psi} &= 2aF_{yf} - 2bF_{rf}, \end{aligned} \tag{5}$$

where $V_x = \dot{x}$ represents the longitudinal vehicle speed.

Using the linear model described by (5) with (3) and (4), the state-space formulation of the model gives:

$$\begin{aligned} \dot{z}(t) &= Az(t) + Bu(t) \\ y(t) &= Cz(t) \end{aligned}, \tag{6}$$

with

$$A = \begin{bmatrix} 0 & 1 & 0 & 0 \\ 0 & -\dfrac{2C_{yf} + 2C_{yr}}{mV_x} & 0 & -V_x - \dfrac{2aC_{yf} - 2bC_{yr}}{mV_x} \\ 0 & 0 & 0 & 1 \\ 0 & -\dfrac{2aC_{yf} - 2bC_{yr}}{IV_x} & 0 & -\dfrac{2a^2C_{yf} + 2b^2C_{yr}}{IV_x} \end{bmatrix},$$

$$B = \begin{bmatrix} 0 \\ \dfrac{2C_{yf}}{m} \\ 0 \\ \dfrac{2aC_{yf}}{I} \end{bmatrix}, C = \begin{bmatrix} 1 & 0 & 0 & 0 \\ 0 & 1 & 0 & 0 \\ 0 & 0 & 1 & 0 \\ 0 & 0 & 0 & 1 \end{bmatrix}$$

and $z=\left[y,\dot{y},\psi,\dot{\psi}\right]^T$ is the state vector, $u=\delta$ and y are the input and the output vector of the model, where δ is the front wheel steering angle. For more details interested readers may refer to [10] and [11].

3. The Mixed Sensitivity Method for H-infinity control design

In control theory, robust control concerns the design of controllers, developed explicitly to account for the process uncertainties.

The "standard" H_∞ optimal control problem is concerned with the feedback system shown in Fig. 2, where w represents the system inputs (setpoint and disturbance), y is the available measurement, u is the control signal, and e is the controlled output. Considering the general case of the multivariable systems, the plant is described by the transfer matrix P, while H is the controller. In H_∞ context, P represents not only the conventional plant to be controlled (considered in what follows as G) but also any weighting functions included to specify the desired performance, which will be discussed later. Suppose that P is partitioned consistent with the inputs w, u and outputs e and y as:

$$P(s)=\begin{bmatrix} P_{11}(s) & P_{12}(s) \\ P_{21}(s) & P_{22}(s) \end{bmatrix} \tag{7}$$

Then, the resulting transfer function of the closed loop is given by:

$$T_{we}=P_{11}+P_{12}H(I-P_{22}H)^{-1}P_{12} \tag{8}$$

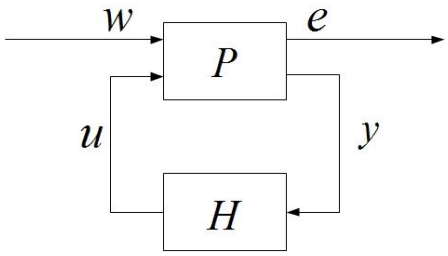

Fig. 2. $H\infty$ feedback control system

It should be reminded that the singular values of a multivariable system, give a measure of the amplitude of the respective system, and enable frequency domain analysis. For SISO systems, the singular values are equivalent with the Bode plot of the system. The H_∞ norm of a given system G is defined as

$$\left\|G\right\|_\infty=\sup_{\omega\in R}\bar{\sigma}(G(j\omega)) \tag{9}$$

where $\bar{\sigma}(A)$ represents the largest singular value of matrix A. Essentially, this means that the H_∞ norm gives a measure of the frequency gain of the system G. Thus the H_∞ control problem is to design the stabilizing controller H, that interacting with the plant, minimizes the H_∞ norm of the closed loop transfer function, i.e. $\left\|T_{we}\right\|_\infty$. This can be achieved by setting a certain threshold $\gamma\in[1,1.5]$ such that $\left\|T_{we}\right\|_\infty\le\gamma$.

One H_∞ control design approach is the "mixed sensitivity" method, and interested readers may refer to [14], [15] and [16]. For simplicity, consider a SISO closed loop system. It is well known that in the closed loop control system can be characterized by the following transfer functions:

$$S(s)=\frac{1}{1+H(s)G(s)} \tag{10}$$

$$R(s)=\frac{H(s)}{1+H(s)G(s)} \tag{11}$$

$$T(s)=\frac{H(s)G(s)}{1+H(s)G(s)} \tag{12}$$

Equation (10) describes the "sensitivity function" of the control system, and (12) describes the overall closed loop transfer function or "complementary sensitivity function".

The H_∞ design approach makes use of the functions described by (10) to (12), by imposing the desired frequency behavior of each of these functions. For example, the performance of a given closed loop system can be specified as requiring:

$$\begin{cases} \left|S(j\omega)\right|\le\varepsilon,\ \forall\omega\le\omega_0 \\ \left|S(j\omega)\right|\le M,\ \forall\omega>\omega_0 \end{cases} \tag{13}$$

where S is given by (10). Although this is generally applicable, it is convenient to formulate the same performance criteria using a weight function w given as a transfer function, as follows:

$$\left|w(j\omega)S(j\omega)\right|\le 1,\ \forall\omega$$

with

$$\left|w(j\omega)\right|=\begin{cases} 1/\varepsilon,\ \forall\omega\le\omega_0 \\ 1/M,\ \forall\omega>\omega_0 \end{cases}$$

Applying such weighting functions on all the transfer functions (10) to (12), the closed loop performance of the system can be specified and tuned.

Considering such weighting functions, the original plant that needs to be controlled can be augmented for the H_∞ control design. The obtained closed loop structure, for the augmented plant can be seen in Fig. 3.

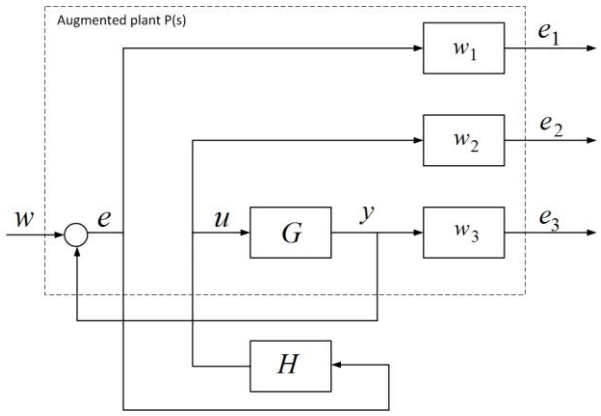

Fig. 3. $H\infty$ closed loop with augmented plant

Having the performance specifications of the closed loop system in time domain, the equivalent specifications from frequency domain can be derived. Based on these frequency specifications, the weighting functions can be designed as follows:

$$w_1(s) = \left(\frac{s / \sqrt[k]{M_s} + \omega_b}{s + \omega_b \sqrt[k]{\varepsilon_1}} \right)^k \tag{14}$$

$$w_2(s) = \left(\frac{s + \omega_{bc} / \sqrt[k]{M_u}}{\sqrt[k]{\varepsilon_2}\, s + \omega_{bc}} \right)^k \tag{15}$$

$$w_3(s) = \left(\frac{s + \omega_{bT} / \sqrt[k]{M_T}}{\sqrt[k]{\varepsilon_3}\, s + \omega_{bT}} \right)^k \tag{16}$$

where, ω_b is the system bandwidth, M_s is the peak sensitivity, ω_{bc} is the controller bandwidth, M_u is the peak gain of the controller, ω_{bT} is the closed loop bandwidth, and M_T is the peak gain of the closed loop system. $\varepsilon_1, \varepsilon_2$ and ε_3 need to be set to small values. Increasing the parameter $k \in \mathbb{R}^*$ results in a steeper rolloff of the frequency response of each weighting function.

The function w_1 is used to weight S, w_2 is used to weight R and w_3 is used to weight T, as follows:

$$|S(j\omega)| \le \frac{1}{|w_1(j\omega)|} \tag{17}$$

$$|R(j\omega)| \le \frac{1}{|w_2(j\omega)|} \tag{18}$$

$$|T(j\omega)| \le \frac{1}{|w_3(j\omega)|} \tag{19}$$

Taking into account the weighting functions (14), (15) and (16), the plant described by (7) can be written in the following form:

$$P(s) = \left[\begin{array}{c|c} w_1 & -w_1 G \\ 0 & w_2 \\ 0 & w_3 G \\ \hline I & G \end{array}\right] \tag{20}$$

By applying (8) to (20) it is obtained

$$T_{we} = \begin{bmatrix} w_1 S \\ w_2 R \\ w_3 T \end{bmatrix} \tag{21}$$

thus, the H_∞ control problem becomes $\left\| \left[w_1 S,\, w_2 R,\, w_3 T \right]^T \right\|_\infty \le \gamma$.

The solution of the H_∞ control problem is based on a state space representation of the generalized plant P, which includes also the weighting functions:

$$\begin{aligned} \dot{x} &= Ax + B_1 w + B_2 u \\ e &= C_1 x + D_1 w + D_2 u \\ y &= C_2 x + D_3 w + D_4 u \end{aligned} \tag{22}$$

The calculation of the controller can then be made by using Riccati approach or the LMI approach, see [14],[15]. Under certain assumptions of controller existence and simplicity, which are skipped here for brevity, the following theorems can be formulated.

Theorem 1: There exists a controller H such that $\|T_{we}\|_\infty \le \gamma$, if and only if:

(1) the matrix $\begin{bmatrix} A & \gamma^{-2} B_1 B_1^T - B_2 B_2^T \\ -C_1^T C_1 & -A^T \end{bmatrix}$ has no eigenvalues on the imaginary axis;

(2) there exists $X_\infty > 0$ such that

$X_\infty A + A^T X_\infty + X_\infty (\gamma^{-2} B_1 B_1^T) X_\infty + C_1^T C_1 = 0$;

(3) the matrix $\begin{bmatrix} A^T & \gamma^{-2} C_1^T C_1 - C_2^T C_2 \\ -B_1 B_1^T & -A \end{bmatrix}$ has no eigenvalues on the imaginary axis;

(4) there exists $Y_\infty > 0$ such that

$$AY_\infty + Y_\infty A^T + Y_\infty(\gamma^{-2}C_1^T C_1 - C_2^T C_2)Y_\infty + B_1 B_1^T = 0;$$

(5) the spectral radius $\rho(X_\infty Y_\infty) < \gamma^2$.

Theorem 2: If the necessary and sufficient conditions of Theorem 1 the obtained controller has the following form:

$$H = \left[\begin{array}{c|c} A_\infty & -Z_\infty L_\infty \\ \hline F_\infty & 0 \end{array}\right] \tag{23}$$

where

$$\begin{aligned} F_\infty &= -B_2^T X_\infty \\ L_\infty &= -Y_\infty C_2^T \\ Z_\infty &= (I - \gamma^{-2} Y_\infty X_\infty)^{-1} \\ A_\infty &= A + B_1 B_1^T X_\infty \gamma^{-2} + B_2 F_\infty + Z_\infty L_\infty C_2 \end{aligned} \tag{24}$$

4. Nonlinear model predictive control

The model based predictive control (MPC) is a digital feedback control approach which is based on predicting the controlled system output over a future horizon (prediction horizon) and calculating the optimal control sequence that will drive the predicted system output as close as possible to the future reference trajectory. The predictions of the future outputs are done virtually in the controller, using a mathematical model of the system, and the optimal control sequence is calculated using an optimization algorithm which minimizes a given cost function.

At each sampling time t (discrete time instant) the controller will predict the future outputs of the system $y(t+k\,|\,t), k = 1, 2, ..., N$ where N is defined as the "prediction horizon". This prediction is employed by simulating internally the system model, using the system states gathered up to the current sample time and the future control signals $u(t+k\,|\,t), k = 1, 2, ..., N$. The future control signals are obtained by minimizing a cost function defined in such a way that the system output will follow as close as possible the reference trajectory $w(t+k\,|\,t), k = 1, 2, ..., N$ and additionally satisfy predefined constraints. A graphical representation of the MPC strategy is presented in Fig. 4.

At each sampling time, only the first sample of the control signal $u(t\,|\,t)$ (which is equal to $u(t\,|\,t)$ is actually sent to the physical process, and the entire algorithm is repeated at the next sampling time.

It can be observed that the model based predictive controller integrates two main components - the mathematical model of the controlled system and the optimization algorithm which minimizes the desired cost function. Both these components play an important role in the performance and stability of the closed loop system and they will be treated in what follows.

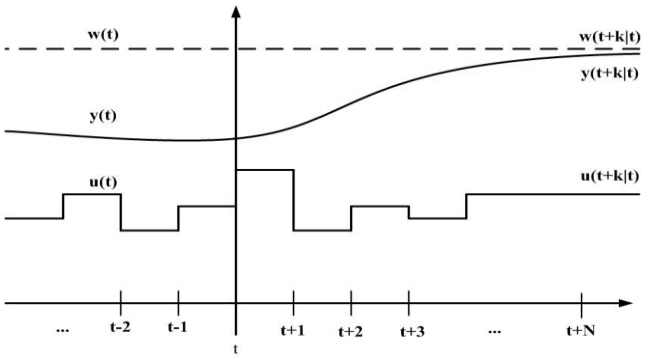

Fig. 4. Model Predictive Control strategy

A. Mathematical model of the controlled system

A nonlinear dynamical system can be modeled by using the ordinary differential equation (ODE):

$$\dot{x}(\tau) = f(x(\tau), u(\tau)) \tag{25}$$

with initial condition:

$$x(0) = x_0 \tag{26}$$

where $x \in R^n$ is the system state vector, $u \in R^m$ is the system input vector and $f : R^n \times R^m \to R^n$ is a nonlinear function which describes the system dynamics. The output of the nonlinear system can be generically defined as:

$$y(\tau) = h(x(\tau), u(\tau)) \tag{27}$$

where $y \in R^r$ is the system output vector and $h : R^n \times R^m \to R^r$ represents a linear or nonlinear mapping of the input and states to the output of the system. In equation (25) and equation (27), $\tau \in R_+$ represents the independent continuous time variable.

Using numerical integration algorithms, also known as ODE solvers, a numerical approximation of the solution of equation (25) is obtained as:

$$x(t+1) = f_d(x(t), u(t)) \tag{28}$$

where t represents the discrete time variable, and $f_d : R^n \times R^m \to R^n$ is a discrete approximation of the nonlinear function defined in (25). The initial condition of this numerical approximation is the same as the initial condition of the differential equation, which is given by (26), and the system output is thus approximated as:

$$y(t) = h(x(t), u(t)) \tag{29}$$

There is a wide range of numerical integration algorithms that can be used in order to obtain the approximation given by (28), and interested readers may refer to [17].

The approximation given by (28) and (29) will be used at each sampling time internally in the controller. The starting point (initial condition) of each simulation, at each sample time will be set to the actual (measured) values of the states of the physical process.

This type of control system is especially attractive for applications in autonomous vehicle steering due to its "predictive" behavior, being able to take into account also the future shape of the desired vehicle path. On the other hand it is intuitive that in order to obtain good performance of the closed loop system, the mathematical model of the system needs to be found as accurate as possible, this representing a big drawback of the NMPC because accurate mathematical models are difficult to develop.

Detailed descriptions of the nonlinear system model and integration in the predictive controller can be found in [18].

B. Optimization algorithm

The role of the optimization algorithm is to search for the optimal control signal which minimizes a predefined cost function of the form:

$$J_N(y,x,u)=\sum_{k=1}^{N} l(y(t+k\mid t),x(t+k\mid t),u(t+k\mid t)) \qquad (30)$$

where the function l can be nonlinear, but usually it is chosen in a quadratic form, including the error between the reference trajectory and predicted output. Equality and inequality constraints on the system states x, output y and control signal u can also be considered in the form:

$$c_i(y(t+k\mid t),x(t+k\mid t),u(t+k\mid t))=0 \qquad (31)$$

$$c_j(y(t+k\mid t),x(t+k\mid t),u(t+k\mid t))\geq 0 \qquad (32)$$

where c_i and c_j can be linear or nonlinear functions.

As the cost function (30) includes the difference between the future reference and predicted output, the optimization algorithm will generate the optimal control signal u which will drive the system model output y as close as possible to the desired reference trajectory w over the prediction horizon N. Thus the optimization operation becomes an optimal control problem, over the prediction horizon:

$$\min_u J_N(y,x,u) \qquad (33)$$

subject to constraints (31), (32), and $x(t)$ and $y(t)$ are given by (28) and (29) over the prediction horizon N.

The minimization of the cost function can be done iteratively, using numerical algorithms of linear, quadratic or nonlinear programming. Interested readers may refer to [20] for details regarding the most frequently employed minimization algorithms and to [18] for detailed aspects regarding the integration in the NMPC approach.

Another advantage of the NMPC can be seen, as it inherently achieves optimal control. A compromise between performance, stability, robustness and computational costs needs to be found in the implementation of the NMPC strategy as it can become computationally expensive.

5. Implementation and Simulation Results

In order to obtain a valid comparison of the two proposed control systems, the same vehicle model was used. The parameters of the vehicle are given in Table 1.

Symbol	Description	Value
m	vehicle mass	$1462\,[kg]$
I	vehicle moment of inertia	$2149\,[kg\cdot m^2]$
a	distance from front axle to center of gravity	$1.108\,[m]$
b	distance rear front axle to center of gravity	$1.392\,[m]$
C_{yf}	front tire stiffness coefficient	$63291\,[N/rad]$
C_{yr}	rear tire stiffness coefficient	$50041\,[N/rad]$

Table 1. Vehicle parameters

The implementation and simulation of both control systems was done in Matlab/SIMULINK software package which provides various tools for H_∞ and NMPC control designing.

The test maneuver was considered similar to a double lane change, precisely starting at position (0,0) in an inertial XY frame, with zero heading angle, the vehicle drives forward for $4\,[\text{sec}]$. At time $t=4\,[\text{sec}]$, the vehicle steers to the left (increasing Y direction) whit a constant steering speed until $t=6\,[\text{sec}]$. The similar steering maneuver is then applied in the opposite direction such that the vehicle will realign parallel with the X axis after $2\,[\text{sec}]$. A forward driving segment is required until time $t=12\,[\text{sec}]$, when a similar steering maneuver is started in the opposite direction (decreasing Y) such that the vehicle will realign to the initial lateral displacement at time $t=14\,[\text{sec}]$.

This maneuver is given in form of a desired trajectory of the vehicle, which can be obtained by using a trajectory planning algorithm which usually is able to calculate the future desired trajectory of the vehicle. These algorithms will not be discussed in this work, and remain subjects for further work.

5.1. H_∞ control implementation

For implementing the proposed H_∞ controller of autonomous vehicle steering, the linear vehicle model was used, while the closed loop validation is done by using the actual nonlinear model of the vehicle. The vehicle model is liniarized at constant vehicle speed of $V_x = 15\left[km/h\right]$ and $V_x = 28\left[km/h\right]$. The control signal of the autonomous steering system is the front wheels steering angle δ, and the output is the lateral position y as presented in the second section of the paper. The sensitivity function (10) and complementary sensitivity function (12) were considered, where $\omega_b = 15\left[rad/\sec\right]$, $\omega_{bT} = 55\left[rad/\sec\right]$, $\varepsilon_1 = 0.001$, $\varepsilon_3 = 0.0001$ and $M_s = M_T = 1.9$. The Bode plot of inverse of the considered weighting functions, which are penalizing the sensitivity and complementary sensitivity functions as seen in (17) and (19), can be seen in Fig. 6. Considering $\gamma = 1.18$, the obtained closed loop transfer function gives the Bode plot shown in Fig. 7. As it can be seen, the closed loop transfer function T_{we} is complying with the specified requirement described $\left\|T_{we}\right\|_\infty \le 1.18$. Also the sensitivity and complementary sensitivity functions are shown in Fig. 7 and Fig. 8, where it can be seen that (17) and (19) are satisfied.

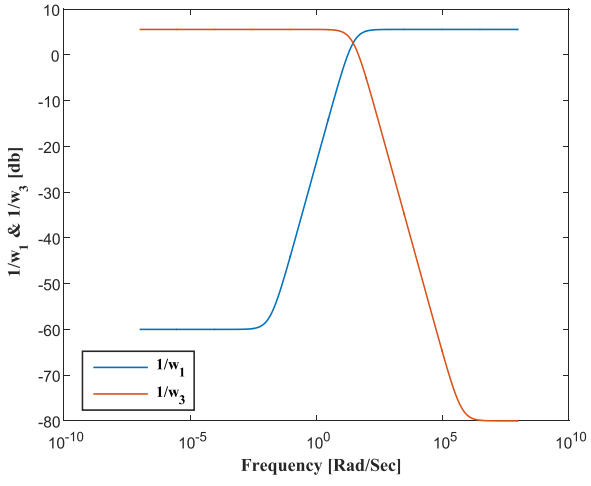

Fig. 5. Bode plot of the inverse of the considered sensitivity functions

Finally, a six order H_∞ controller is found, that stabilizes the vehicle lateral dynamics and fulfils the closed loop specifications. The transfer function of the controller was obtained:

$$H(s) = \frac{(-4159E-05)s^5 + 127.1s^4 + 8.247E07s^3 + 3.356E09s^2 + 3.408E10s + 0.1074}{s^5 + 5101s^4 + 2.201E06s^3 + 3.706E08s^2 + 5.07E09s + 7.596E07}$$

The *Robust Control Toolbox* [21] function set was used for this design.

A simulation of a double lane change maneuver is presented in Fig. 10, in order to analyze the trajectory tracking of the closed loop control system for the automatic vehicle.

As it can be seen from Fig. 10, where were carried out also at different vehicle speeds $V_x = 15\left[km/h\right]$ the proposed H_∞ control system is performing very well in vehicle trajectory tracking applications, obtaining a very small tracking error.

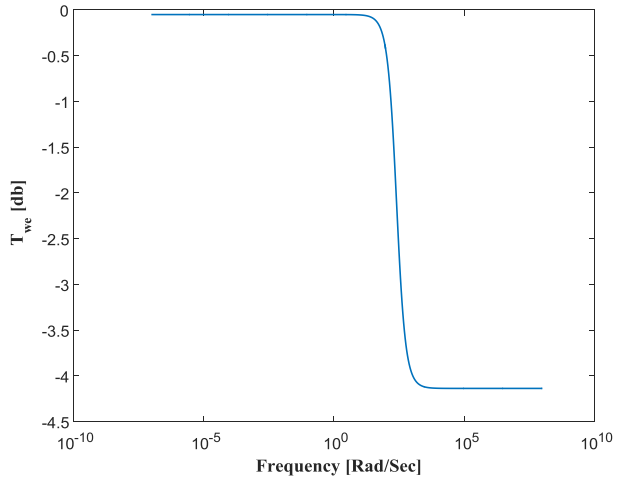

Fig. 6. Bode plot of the closed loop transfer function

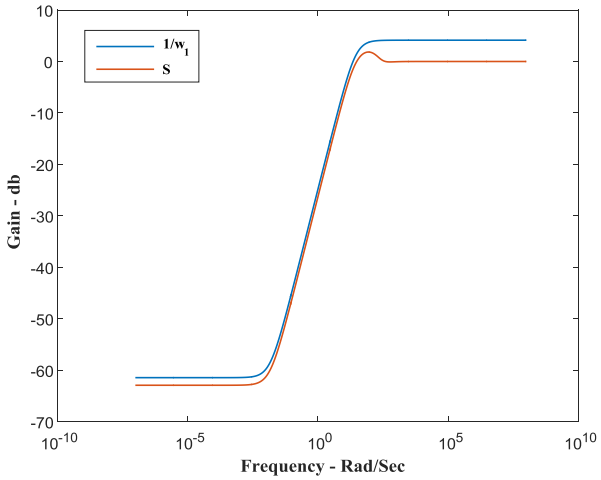

Fig. 7. Comparison of $1/w_1$ and S

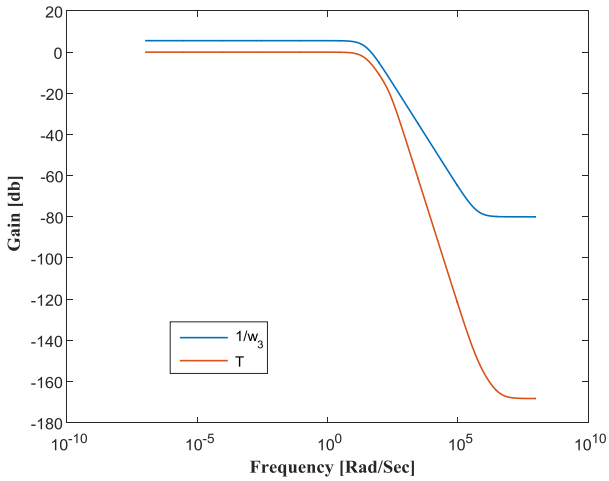

Fig. 8. Comparison of $1/w_3$ and T

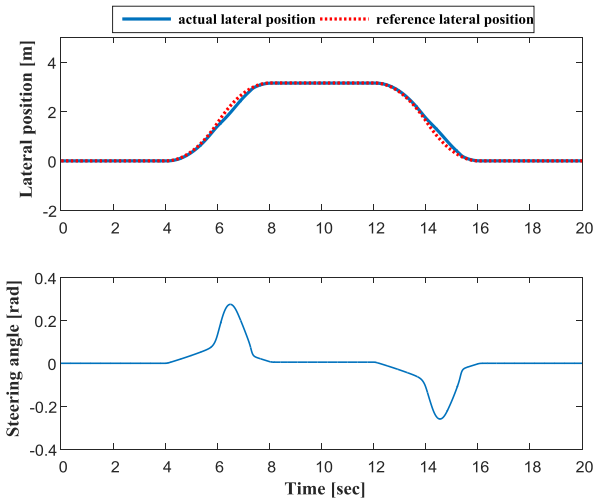

Fig. 9. Double lane change maneuver of H_∞ at $V_x = 15\left[km/h\right]$

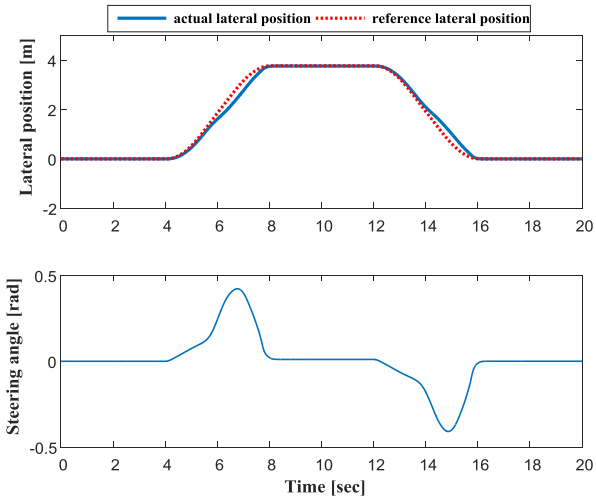

Fig. 10. Double lane change maneuver of H_∞ at $V_x = 28\left[km/h\right]$

Simulations were carried out also at different vehicle speeds $V_x = 28\left[km/h\right]$. In Fig. 11 it can be seen that the automatic steering maneuvers are still performed with sufficiently high accuracy, showing that the H_∞ controller is robust.

5.2. Nonlinear model predictive control implementation

As described in Section 4, in order to implement the nonlinear predictive controller for the vehicle steering an adequate vehicle model which captures as accurate as possible the vehicle dynamics needs to be used. A widely used model in industry and literature is the single track vehicle model (or bicycle model) [19], [10]. This model captures the most important dynamics and nonlinearities of the vehicle, and it will also be used in this study.

In what follows the vehicle modelling using the single track model and the optimal control problem used for the design of the nonlinear predictive control of vehicle steering will be presented.

C. Vehicle lateral dynamics model

The nonlinear vehicle model is considered only for the lateral dynamics which is described by (5).

The main external influences in the vehicle lateral dynamics described by the proposed vehicle model are given by the tire forces F_{yf} and F_{yr}, which are highly nonlinear and have a high impact in vehicle maneuvering. Although in the H_∞ control design these forces were considered linear, by assuming small slip angles (see equation (3)), the NMPC approach gives the possibility to incorporate a nonlinear and more realistic model for the tire forces F_{yf} and F_{yr}. The tire model used in this study is the Pacejka tire model or also known as *Magic Formula* tire model [13].

This model is a semi-empirical model, which was continuously improved over the years, developed based on experimental results. One of the earliest versions of this model describes the lateral tire force as:

$$F_y = D\sin\{C\tan^{-1}[B(1-E)\alpha + E\tan^{-1}(B\alpha)]\} \qquad (34)$$

where

$$D = a_1 F_z^2 + a_2 F_z \qquad (35)$$

$$C = 1.3 \qquad (36)$$

$$B = \frac{a_3 \sin[a_4 \tan^{-1}(a_5 F_z)]}{CD} \qquad (37)$$

$$E = a_6 F_z^2 + a_7 F_z + a_8 \qquad (38)$$

Equation (34) provides the tire lateral force based on the tire slip angle α and on the normal force F_z trough the parameters B, C, D and E.

The tire slip angle for the front and rear wheels, respectively, can be calculated using (4)

The normal forces used in (35), (37) and (38) are considered to be constant, and are given for the front and rear wheels as:

$$F_{zf} = \frac{bmg}{2(a+b)} \tag{39}$$

$$F_{zf} = \frac{amg}{2(a+b)} \tag{40}$$

where represents the gravitational constant.

The parameters $a_1, a_2, ..., a_8$ used in (35), (37) and (38) are chosen based on the values of F_{zf} and F_{zr} as explained in [13].

The resulting model, using the equations (5) and (34) trough (40) describes the vehicle lateral dynamics, considering as input the steering angle of the front wheel δ and as output the vehicle lateral position y (with respect to the lateral axis of the inertial frame-Y).

This model will be further used in the control system design.

D. Optimal control problem

For solving the optimal control task, the cost function defined in (30) was chosen in the simple form as:

$$J_N = \sum_{k=1}^{N} [w(t+k \mid t) - y(t+k \mid t)]^2 \tag{41}$$

This cost function is often used in predictive control applications.

No constraints were defined for the cost function (41) in this work. The optimal control problem is now given as:

$$\text{find} \ \min_{u} J_N \tag{42}$$

subject to:

$$y(k+1) = f_{vd}(y(k), \psi(k), \delta(k)), \ y(0) = y_0 \tag{43}$$

where represents the vehicle lateral position, ψ represents the vehicle yaw angle and δ is the front wheel steering angle. f_{vd} is the approximation of the vehicle model defined by (5) and (34) obtained using the built in ODE solver *ode45* provided by Matlab [22].

The minimization of the objective (42), (43) is executed at each sample time using the *fmincon* function with SQP (Sequential Quadratic Programming) algorithm which is provided in Matlab. Details regarding this minimization algorithm can be found in [20]. At each time instant, the optimal control problem (42), (43) will be solved and the new generated optimal control sequence (front wheel steering angle) will be sent to the vehicle. It needs to be noted that only the first sample of the control signal $\delta(t \mid t)$ will be actually applied, and the rest of the control sequence ($\delta(t+k \mid t), k = 1, 2, ..., N$) will be used in the next sample time as initial guess for the optimization algorithm.

The obtained closed loop structure is depicted in Fig. 5, where $w(t+k \mid t), k = 1, 2, ..., N$ represents the future desired lateral position, $\delta(t+k \mid t), k = 1, 2, ..., N$ represents the future steering angle, $y(t+k \mid t), k = 1, 2, ..., N$ is the future predicted lateral position, $\varepsilon(t+k \mid t) = w(t+k \mid t) - y(t+k \mid t)$, $k = 1, 2, ..., N$ is the future lateral position tracking error, $\delta(t) = \delta(t \mid t)$ and $y(t) = y(t \mid t)$ are the actual applied steering angle and the obtained lateral position. The cost function (41). used by the optimization algorithm

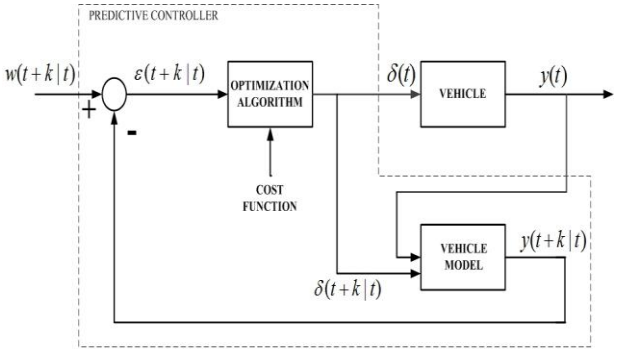

Fig. 11. Nonlinear predictive control of vehicle lateral dynamics

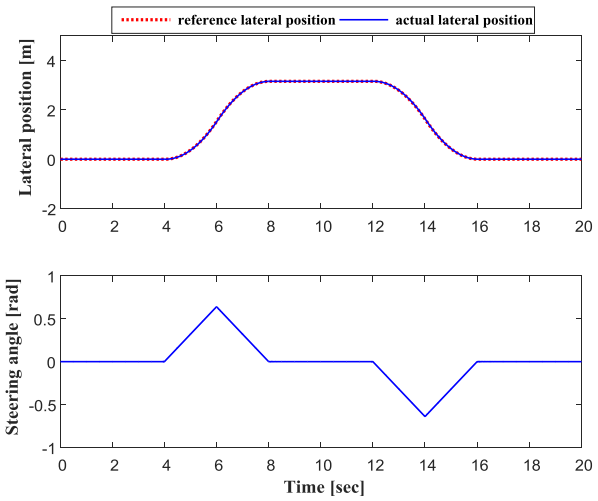

Fig. 12. Double lane change maneuver of NMPC at $V_x = 15 \left[km/h \right]$

Similar simulations of double lane change maneuvers were carried out for the nonlinear predictive controller. In Fig. 12 it can be seen the simulation at $V_x = 15\left[km/h\right]$ while in Fig 13. the simulation at $V_x = 28\left[km/h\right]$ is presented. The prediction horizon was chosen $N = 10$, and increasing this value will yield a even better performance.

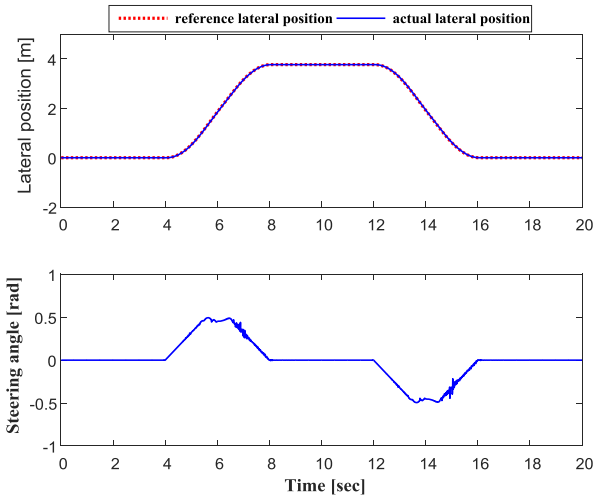

Fig. 13. Double lane change maneuver of NMPC at $V_x = 28\left[km/h\right]$

7. Conclusions

As it can be seen from the simulation results, the proposed NMPC strategy is giving better trajectory tracking results in comparison with the H_∞. The advantage of the NMPC is that it incorporates optimal control and can take into account the nonlinearities of the vehicle model. It also can be seen from the simulation results that the NMPC obtained a steering angle waveform similar as described in the beginning of Section 5 due to the incorporation of optimal control. At the same time, closed loop stability needs to be carefully considered, and although this paper does not touch this subject, usually additional measures need to be taken in order to ensure stability of the NMPC strategy, for example active or terminal constraints. The H_∞ controller ensures the stability around the functioning states where the vehicle model was linearized, and is robust enough for controlling when the vehicle speed is higher than the vehicle speed considered for linearization. For covering a full speed range, a gain scheduling strategy can be adopted for H_∞ strategy. A disadvantage of the H_∞ control is that the degree of the controller can get very high, as is also the case in this work and this is usually avoided in the automotive industry, due to real-time implementation on embedded systems.As future work, further comparison analysis will be made concerning the stability of both controllers and performances in disturbance rejection or unfavorable road conditions.

Acknowledgment

This paper was supported by a grant of the Romanian National Authority for Scientific Research and Innovation, CNCS – UEFISCDI, project number PN-II-RU-TE-2014-4-0970.

References

1. Ü. Özgüner, T. Acarman, and K. Redmill, Autonomous ground vehicles, Artech House, 2012.
2. M. Amoozadeh, H. Deng, C. N. Chuah, H. M. Zhang, D. Ghosal, Platoon management with cooperative adaptive cruise control enabled by VANET, Vehicular Communications, Vol. 2, Issue 2, 2015.
3. T. C. Martin, M. E. Orchard, P. V. Sanchez, Design and Simulation of Control Strategies for Trajectory Tracking in an Autonomous Ground Vehicle, IFAC Conference on Management and Control of Production, Fortaleza, Brazil, 2013.
4. C. Hu, H. Jing, R. Wang, F. Yan, M. Chadli, Robust H_∞ output-feedback control for path following of autonomous ground vehicles, Elsevier Mechanical Systemsand Signal Processing, 2016.
5. R. Wang, H. Jing, C. Hu, M. Chadli, F. Yan, Robust H_∞ output-feedback yaw control for in-wheel motordriven electric vehicles with differential steering, Elsevier Neurocomputing, 2016.
6. A. Carvalho, S. Lefévre, G. Schildbach, J. Kong, and F. Borrelli, Automated driving: The role of forecasts and uncertainty - A control perspective, European Journal of Control, Vol. 24, pp. 14–32, 2015.
7. R.C. Rafaila, and G. Livint, Nonlinear Model Predictive Control of Autonomous Vehicle Steering, 19th International Conference on System Theory, Control and Computing, Cheile Gradistei, Romania, 2015.
8. R. C. Rafaila, C. F. Caruntu, G. Livint, Nonlinear Model Predictive Control using Lyapunov Functions for Vehicle Lateral Dynamics, IFAC Symposium on Control in Transportation Systems, Istanbul, Turkey, May 18-20, 2016.
9. P. Falcone, M. Tufo, F. Borrelli, J. Asgari, and H. E. Tseng, A Linear Time Varying Model Predictive Control Approach to the Integrated Vehicle Dynamics Control Problem in Autonomous Systems, 46th IEEE Conference on Decision and Control, New Orleans, Los Angeles, USA, pp. 2980 - 2985, 2007.
10. R. Rajamani, Vehicle Dynamics and Control, chapters 2 and 4, Springer Verlag, 2nd ed., 2012.
11. B. Heissing, M. Ersoy, Chassis Handbook, Vieweg + Teubner Verlag, 1st ed., 2011.
12. H. Pacejka, Tire and Vehicle Dynamics, chapters 1,2,4, Elsevier Ltd, 3rd ed, 2012.
13. H. B. Pacejka, E. Bakker, and L. Nyborg, Tyre Modelling for Use in Vehicle Dynamics Studies, Society of Automotive Engineers, 1987.
14. S. Skogestad and I. Postlethwaite, Multivariable Feedback Control: analysis and design, John Wiley and Sons, 2005.
15. K. Zhou, Essentials of Robust Control, Prentice Hall, New Jersey, 1998.
16. I. M. T. Birou, Robust Control of Sensorless AC Drives Based on Adaptive Identification, Recent Advances in Robust Control - Theory and Applications in Robotics and Electromechanics, Intech, November, 2011.
17. A. R. Krommer, C. W. Ueberhuber, Numerical Integration on Advanced Computer Systems, Lecture Notes in Computer Science, Springer, 1994
18. L. Grüne, J. Pannek, Nonlinear Model Predictive Control, Springer, 2011.
19. T. Keviczky, P. Falcone, F. Borrelli, J. Asgari and D. Hrovat, Predictive Control Approach to Autonomous Vehicle Steering, In

Proceedings of the 2006 American Control Conference, Minneapolis, MN, June, 2006.

20. J. Nocedal, S. J. Wright, Numerical Optimization, Springer, 2nd ed, 2006.
21. G. Balas, R. Chiang, A. Packard, M. Safonov, Robust Control Toolbox User's Guide, (https://www.mathworks.com/help/pdf_doc/robust/robust_ug.pdf).
22. F.S. Lawrence, M.W. Reichel, The Matlab Ode Suite, (https://www.mathworks.com/help/pdf_doc/otherdocs/ode_suite.pdf).